

# RSC Advances

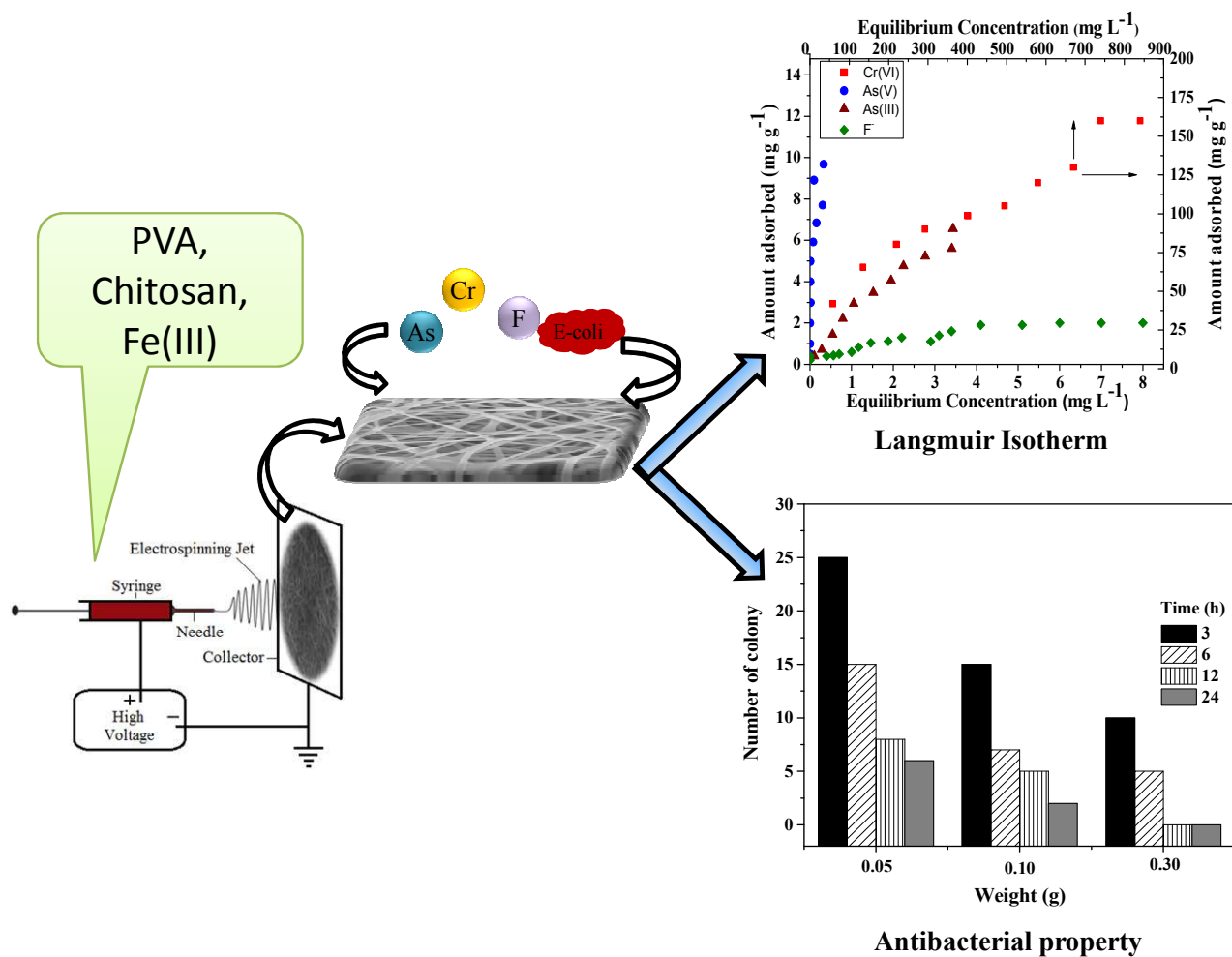


This is an *Accepted Manuscript*, which has been through the Royal Society of Chemistry peer review process and has been accepted for publication.

*Accepted Manuscripts* are published online shortly after acceptance, before technical editing, formatting and proof reading. Using this free service, authors can make their results available to the community, in citable form, before we publish the edited article. This *Accepted Manuscript* will be replaced by the edited, formatted and paginated article as soon as this is available.

You can find more information about *Accepted Manuscripts* in the [Information for Authors](#).

Please note that technical editing may introduce minor changes to the text and/or graphics, which may alter content. The journal's standard [Terms & Conditions](#) and the [Ethical guidelines](#) still apply. In no event shall the Royal Society of Chemistry be held responsible for any errors or omissions in this *Accepted Manuscript* or any consequences arising from the use of any information it contains.



Graphical Abstract



Journal Name

[Dynamic Article Links ►](#)

Cite this: DOI: 10.1039/c0xx00000x

[www.rsc.org/xxxxxx](http://www.rsc.org/xxxxxx)

ARTICLE TYPE

## Facile synthesis of smart biopolymeric nanofibers towards toxic ions removal and disinfection control

Divya Chauhan,<sup>a,b</sup> Jaya Dwivedi<sup>b</sup>, Nalini Sankararamkrishnan<sup>\*,d</sup>

Received (in XXX, XXX) Xth XXXXXXXXX 20XX, Accepted Xth XXXXXXXXX 20XX

DOI: 10.1039/b000000x

To provide safe drinking water, it is inevitable to tackle both bacterial infection and inorganic pollutants. In this study a smart biopolymeric nanofibers consisting of Chitosan/Fe(III)/PVA (CPF) by electrospinning method have been synthesized. Cross linking with glutaraldehyde was carried out to increase the stability of the mats. The prepared CPF mat exhibited increased adsorption sites facilitating the removal of As(III), As(V), Cr(VI) and F<sup>-</sup> ions. The selectivity order of the investigated anions towards CPF mats followed the sequence Cr(VI) > As(V) > As(III) > F. Maximum adsorption capacities of Cr(VI), As(V), As(III) and F were found to be 166.7, 83.3, 32.3 and 2.5 mg/g respectively. The prepared CPF mat also exhibited 100% disinfection towards *e coli* at an initial concentration of 10<sup>4</sup>-10<sup>5</sup> CFU/ml. Using FTIR studies mechanism of interaction of these ions with CPF have been postulated.

### 1. Introduction

In developing countries like India, owing to the rapid growth of human population and industrialization, the concerns over water contamination have become a critical issue. To provide safe drinking water, both chemical and bacteriological contaminants need to be addressed. To augment biological contamination, water treatment plants often use procedures such as chlorination, ozonolysis, UV irradiation and electromagnetic radiation. It is well known that during chlorination formation of disinfection by products is of serious concern<sup>1</sup>. Thus, the important challenge faced by the nation is an efficient and cost-effective method for water purification without endangering human health. In recent years, removal of toxic ions such as Cr(VI), As(III), As(V) and Fluoride are challenging owing to their high toxicity. The current permissible limits of U.S. EPA for these ions are 100 ppb for Cr(VI), 10 ppb for inorganic arsenic, and 4.0 ppm for fluoride<sup>2</sup>. Among the commonly used methods such as flocculation, sedimentation, filtration, reverse osmosis and adsorption for the removal of these toxic ions, adsorption is advantageous owing to cost effectiveness and the amount of sludge generated is also less. Among the several types of adsorptive materials used for the control of these toxic ions in water, activated alumina<sup>3</sup>, activated carbon<sup>4</sup> are the extensively studied adsorbents. However, these

adsorbents are inefficient to remove the contaminants down to parts per billion level<sup>5</sup> and additional treatment methods are required to circumvent biological contamination. Thus in an effort to tackle both chemical and biological contamination, chitosan a biopolymer was chosen. Chitosan is a biodegradable, non-toxic polysaccharide derived from naturally occurring chitin. Chitin is the second most abundant polysaccharide found in the exoskeleton of crustaceans, shrimp and crab shells, insects and fungal mycelia<sup>6</sup>. Chitosan is a copolymer of N-acetyl-D-glucosamine and D-glucosamine, and the D-glucosamine content is dependent on the degree of deacetylation (DDA) of chitin to chitosan. It has many attractive features such as hydrophilicity, biodegradability, biocompatibility and antibacterial properties. It has been proved to be effective in removing various metal ions owing to the presence of amino and hydroxyl groups on its backbone<sup>6</sup>. The antibacterial properties of chitosan could be attributed to the electrostatic interaction between the positively charged amine groups on the chitosan backbone and negatively charged components in the microbial cell membranes. Binding between cell wall components and chitosan alters the barrier properties and leads to cell death<sup>7</sup>. In recent years, nano fibers have attracted wide attention owing to high surface area, porosity and good permeability. These nanofibrous mats are used in wide range applications across environmental areas such as removal of heavy metal and pathogens<sup>8-11</sup> although their full potential in environmental applications has not been systematically explored. Recently, Mahanta and Valiyaveetil<sup>12</sup> revealed the use of Fe(III) loaded PVA fibres towards the removal of arsenic and reported a capacity of 36 and 67 mg g<sup>-1</sup> for As(V) and As(III) respectively. Though the capacity towards arsenic was good its application towards biological contamination and other toxic metal ions needs to be explored. Few reports are available in the literature on the use of chitosan mats for the removal of copper and lead ions<sup>9</sup> and *e coli* bacteria<sup>8</sup>. Nano zerovalent iron supported chitosan fibre was evaluated by Horzum et. al.<sup>13</sup> for the removal of arsenic. The main disadvantages of this fibre being the usage of toxic solvent like pentafluoro isopropanol during spinning process. Green environment friendly nanofibres, was synthesized using a composite consisting of zerovalent iron/chitosan/PVA and its applicability towards arsenic removal has been demonstrated<sup>14</sup>. The afore mentioned methods have been successfully utilized for either heavy metals or bacterial

disinfection. Factors relevant to safe drinking water targeting both the removal efficiency of variety of water contaminants down to ppb range and circumventing microbial contamination were seldom being considered. To address these issues, a green nanocomposite membrane consisting of Fe(III)/PVA/Chitosan was synthesized exhibiting advantageous properties for disinfection control and toxic ion removal and biocompatibility for safe drinking water. The nanofibrous membrane was synthesized by electrospinning technique using chitosan, polyvinyl alcohol and Fe(III) salt. Polyvinyl alcohol acted as stabilizer<sup>15</sup> and enabled smooth spinning of chitosan fibers. The affinity and selectivity of Fe(III) towards inorganic arsenic is well known<sup>14,16</sup>. In addition Fe(III) salts doped chitosan hydrogels have been reported for the removal of Cr(VI) ions<sup>17</sup>. The prepared nanocomposite electrospun nanofibers were systematically characterized using various techniques including SEM, XRD and FTIR, and applied for the removal of various toxic ions such as As(III), As(V), Cr(VI), F and ecoli bacteria. The main novelty of the present work is the comprehensive study on its applicability to variety of toxic ions and circumventing bacterial contamination as well. Further, selectivity studies were also carried out for these electrospun nanofibers.

## 2. Experimental Details

### 2.1. Materials

All the chemicals and chelating agents used in this study such as Chitosan (about 85% deacetylated), Poly vinyl alcohol (PVA) with molecular weight of 1,25,000 g/mol, Ferric nitrate (Fe(NO<sub>3</sub>)<sub>3</sub>), Glutaraldehyde were obtained from Sigma Aldrich. Acetic acid (99.8%) used to dissolve chitosan was obtained from Rankem chemicals. Sodium arsenate (Na<sub>2</sub>HAsO<sub>4</sub>·7H<sub>2</sub>O, Merck) and arsenic oxide (As<sub>2</sub>O<sub>3</sub>, Sigma-Aldrich) were used for preparing the stock solutions of arsenate and arsenite respectively. Chromium, and Fluoride standard solutions were prepared from respective salts of K<sub>2</sub>Cr<sub>2</sub>O<sub>7</sub>, and NaF. Total ionic strength adjustor buffer (TISAB III) solution was acquired from E-Merck India Ltd., Mumbai, India.

### 2.2. Preparation of Chitosan/PVA/Fe solution

The Chitosan (3 % w/v) and PVA (10 % w/v) solutions were initially prepared separately by dissolving Chitosan in 2 % acetic acid and PVA in deionised water at 80°C. Then, Chitosan and PVA solutions were blended in the ratio of 1:1. To this mixture added Ferric nitrate (0.2 gm for 20 ml solution) and the resulting solution containing chitosan/PVA/Fe(III) was stirred for 24h.

### 2.3. Electro spinning process

The prepared Chitosan/PVA/Fe solution was loaded into a 20 mL plastic syringe equipped with a syringe needle having an inner diameter of 0.3 mm. Syringe was placed to a programmable syringe pump (E-spin nano tech) to control the solution flow rate. A positive electrode of high voltage power supply was connected to the syringe needle and a negative electrode was connected to a cylindrical collector covered with aluminum foil which served as a collector. Then, a high voltage was applied between needle and collector so that Chitosan/PVA/Fe nano fibers were produced on the collector. A voltage of 20 kV, with a tip-collector distance of 10 cm, at 5 µL/min speed was applied to the solution and fibers

were collected on the cylindrical collector. Then 2% glutaraldehyde solution was used for cross-linking of Chitosan/PVA/Fe nanofiber membrane render the fibers with water stability<sup>18</sup>. In aqueous medium due to high hydrophilicity of PVA, solubilisation of fibres was observed. The fibers were dried for 24 hrs at 80°C in oven. Thus, to prevent dissolution of PVA and leaching of iron, and increase the stability of both chitosan and PVA electrospun mat, crosslinking was carried out with a dialdehyde, namely glutaraldehyde. In the case of PVA, crosslinking occurs between hydroxyl groups whereas, in chitosan a schiff's base reaction occurs between the amino group of chitosan and aldehydic groups of glutaraldehyde. Scheme 1 depicts the crosslinking of glutaraldehyde with chitosan and PVA.

### 2.4. Characterization of electro spun nano fibres

Images of electro spun nanofibres were obtained with a field emission scanning electron microscope (Carl Zeiss NTS GmbH, Oberkochen (Germany) Model: SUPRA 40VP) operated at an accelerating voltage of 10 kV. Prior to imaging, the samples mounted on copper stubs were coated with gold for better conductivity during imaging. FT-IR spectra were recorded with a Nicolet 17DSX FT-IR Spectrometer. The X-ray diffraction (XRD) patterns of nanofibers were measured using Hecus X-Ray Systems GmbH, Graz (Austria) Model: S3 MICRO.

### 2.5. Performance of the CPF towards toxic ions uptake

Adsorption experiments were carried out by batch technique. Optimum pH for the uptake of these ions were carried out with water containing different toxic ions (Cr(VI) 10.0 mg/L; As(III)/As(V) 2.3 mg/L; F 1.0 mg/L). The initial pH of the solution was varied from 2 – 9 using aqueous solution of NaOH or HCl with 20 mg of CPF mat in a final volume of 20 mL. At the end of the equilibrium time, the content was separated by filtration with 0.22µm pore size filter paper and arsenic in solution was analyzed by inductive coupled plasma-mass spectrometry (ICP-MS) (Thermo Scientific, XSERIES 2) for As(III) and As(V). Analysis of Cr(VI) was carried out diphenyl carbazide method<sup>19</sup>. Analysis of fluoride ion in the filtrates was carried out by fluoride selective electrode using ORION Fluoride meter. During fluoride analysis, addition of total ionic strength adjustment buffer (TISAB) solution eliminated the interference from complexing ions. The electrode was calibrated daily with a series of 5 or more fluoride standard solutions within the linear working range of the fluoride electrode. All the experiments were carried out twice. The amount of the ions adsorbed (mg) per unit mass of CPF (g), *q<sub>e</sub>*, was obtained by mass balance using the following equation:

$$q_e = \frac{(C_i - C_e)}{m} \times V \quad (1)$$

Where *C<sub>i</sub>* and *C<sub>e</sub>* are initial and equilibrium concentrations of the metal ion (mg/L), *m* is dry mass of nanofibre mat (g) and *V* is the volume of the solution (L). The percent extraction efficiency of the sorbent can be calculated by using the following equation:

$$\text{Extraction Efficiency (\%)} = (C_0 - C_e)/C_0 \times 100 \quad (2)$$

For kinetic studies, initial concentration of ions was maintained as described earlier. Except for Cr(VI) where the initial pH was maintained at 3, for all other ions pH was adjusted to 7 and the solutions were equilibrated. Samples were taken at regular intervals and analysed for their respective analyte. For isotherm experiments, about 20 mg of adsorbent (CPF) was placed in a beaker containing 20 mL of 0.1 to 10 mg/L of As(V)/As(III)/F and 100 – 1000 mg/L of Cr(VI) solution and equilibrated. All other parameters were maintained as before and the amount of toxic ions adsorbed was calculated using equation (1).

### 2.5 Antibacterial activity

The antibacterial activity was ascertained for the prepared chitosan/pva (CP) and chitosan/pva/Fe nanofibers (CPF) mat against gram negative *Escherichia coli* (*E.coli*) bacterial strain. *E.coli* (K-12) strain was obtained from national laboratory in India and cultured in Luria-Bertani broth (LB broth) containing tryptone 10 g L<sup>-1</sup>, yeast extract 5 g L<sup>-1</sup>, and NaCl 10 g L<sup>-1</sup> for 24 h at 37°C. The antibacterial analysis was determined by using plate count method in LB agar medium (tryptone 10 g L<sup>-1</sup>, yeast extract 5 g L<sup>-1</sup>, NaCl 10 g L<sup>-1</sup> and agar 15 g L<sup>-1</sup>) and incubated at 37°C for 24 hrs. 1 ml of bacterial culture LB medium was diluted in 50 ml of sterilized DI water. Different weight (0.05 to 0.3 gm) of the mats were added to the bacterial solution and incubated in shaking incubator at 37°C with speed of 120 rpm. Samples (100 µl) were drawn from the incubated conical flask at different time intervals (3, 6, 12, and 24h) and spread onto LB agar plates. The initial bacterial concentration was approximately 10<sup>4</sup>-10<sup>5</sup> CFU/ml. The bacterial solution without CP and CPF nanofibers mat served as control. The antibacterial analysis was carried out for 24 h. The analysis was performed in duplicate to ensure the reproducibility.

## 3. Results and Discussions

### 3.1. Characterization of Nanofibres

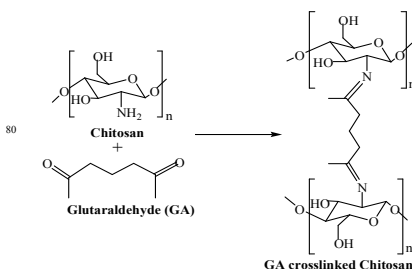
#### 3.1.1 Electron microscopy and Fibre size distribution

The morphology of electro spun nano fibers is influenced by various parameters such as flow rate, applied voltage, tip to collector distance and properties of polymer solutions<sup>20</sup>. The morphology of the chitosan/PVA/Fe electro spun nano fiber mat was characterized by Scanning electron microscope. Figure 1(a) shows the SEM image of as spun Chitosan/PVA/Fe electro spun nano fiber mat which have non beaded fibrous structure and Figure 1(b) shows the SEM image of glutaraldehyde (2% in methanol) cross linked Chitosan/PVA/Fe electro spun nano fiber mat. It was observed that the thickness of fibers present in fibrous mat slightly increases because of hydrophilic character of few untreated alcoholic group of PVA present in fibrous mat. Elemental distribution of fibers mat shown in image 1(a) and (b) confirms the presence of carbon, oxygen and iron in fibrous mat. TEM micrograph (Fig. 1(e) and 1(f)) also supports the non uniform nano fibrous structure of mat. Further it should be noted that Fe is dissolved uniformly in the fibre and absence of iron nano particles even in high resolution TEM (Fig. 1 (f)).

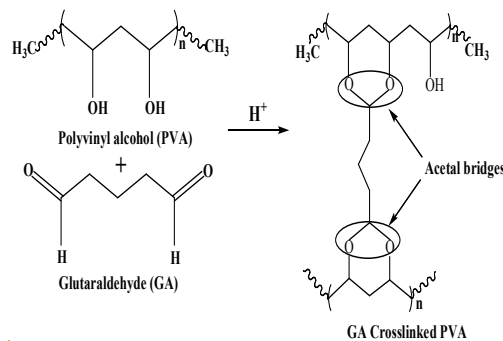
Fibre size distribution (diameter of the fibres) was plotted with the help of image j software<sup>21</sup> and the result obtained is shown in

Fig. 1 (c) and 1 (d). It was evident from Fig. 1(c) that around 59% of the fibres were less than 100 nm and rest 41% of fibre were found to be in range of 100-200 nm which is lesser than pure PVA fibres size as reported in literature<sup>12</sup>. The reduction in fibre size is because of increment of charge density due to addition of chitosan, a cationic polysaccharide, in the electrospinning jet leads to higher elongation forces due to higher conductivity of polymeric solution resulting thinner diameter of fibres<sup>21</sup>. In case of crosslinked fibre mat fibre size distribution was found slightly higher (Fig. 1 (d)). Around 45% of fibres were less than 150 nm and rest 55% of fibres were found to be in range of 150-300 nm. The increment in fibre size is because of hydrophilic character of PVA present in the mat. The porosity of virgin and crosslinked chitosan/PVA/Fe nano fiber mat was found to be 30% and 60% respectively. The lower porosity of the virgin mat in aqueous solution could be attributed to the distorted fibrous structures<sup>14</sup>. The amount of glutaraldehyde used was optimized such that free amino groups exist on the nanofiber for complexation reaction with the metal ions<sup>14</sup>. Further the presence of primary amino groups in CPF was confirmed by FTIR studies which are detailed in Sec 3.1.2.

Chitosan and Glutaraldehyde (GA) crosslinking equation



Polyvinyl alcohol and GA crosslinking equation-



Scheme 1. Cross linking of Chitosan and PVA with Glutaraldehyde

Formatted: Font: 9 pt

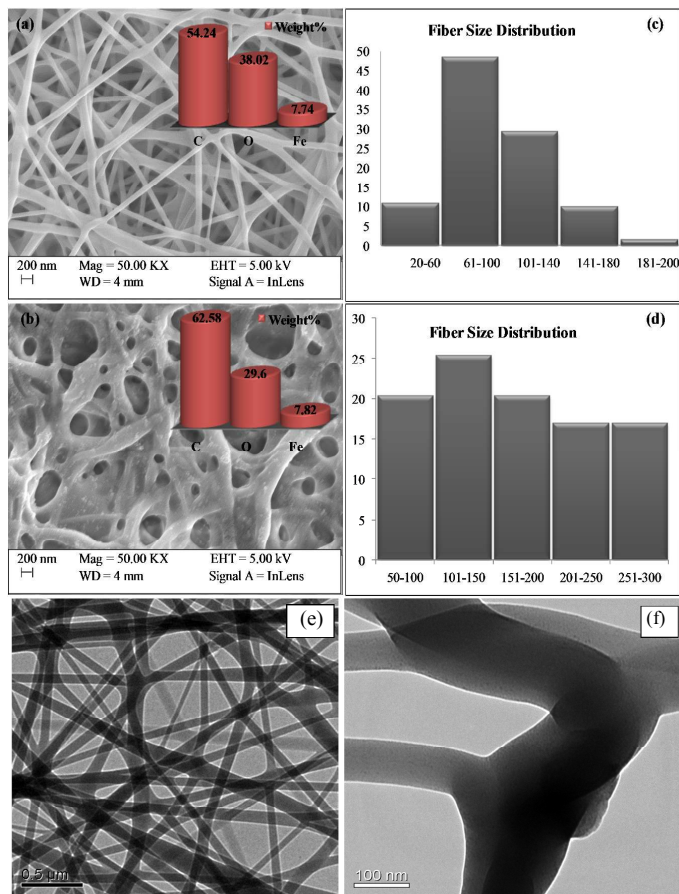


Fig.1 a. SEM image of as spun CPF, b. Glutaraldehyde crosslinked CPF, c. Fibre size distribution of as spun CPF, d. Fibre size distribution of glutaraldehyde crosslinked CPF, e. and f. TEM micrograph of as spun CPF

### 3.1.2 FTIR Spectra

FTIR spectra of unloaded CPF (Fig. 2a) exhibited broad peak at  $3390\text{ cm}^{-1}$  due to superimposition of O-H and  $\text{-N-H}$  vibrations. The C-H stretching vibration of the polysaccharide backbone is manifested through strong peak at  $2923\text{ cm}^{-1}$ . The sharp peak at  $1721\text{ cm}^{-1}$  could be attributed to the C-O stretching vibration. The band at  $1538\text{ cm}^{-1}$  could be attributed to the bending vibration of the free primary amino group on the chitosan backbone. The crosslinking between the aldehydic groups of glutaraldehyde and amino groups of chitosan to form a Schiff base is evident from the peak at  $1634\text{ cm}^{-1}$  which corresponds to  $\text{-C=N}$  vibration. Additional peaks at, 844, 608 and  $469\text{ cm}^{-1}$  confirms the Fe-OH structural vibration<sup>23</sup>. The changes observed in FTIR spectra after As(V) and As(III) loading is also shown in Fig. 2a. After metal

ion loading the peak at  $3390\text{ cm}^{-1}$  is suppressed which might be attributed to the interaction of arsenic ions with the functional groups present in the chitosan ( $\text{-OH}$  and  $\text{-NH}_2$ ). Due to the complexation of Fe(III) with As(III)/As(V) to form ferric arsenite or ferric arsenate changes in Fe-OH vibration is observed. In the case of As(V), a peak shift from  $844$  to  $830\text{ cm}^{-1}$  and  $608$  to  $603\text{ cm}^{-1}$  is observed<sup>24</sup>. However after As(III) loading a peak at  $836$  is observed due to the formation of ferric arsenite<sup>25</sup>. In Fig. 2b a peak at  $1538\text{ cm}^{-1}$  corresponding to  $\text{NH}_3^+$  is diminished after fluoride loading owing to the strong electrostatic attraction between positive charged  $\text{-NH}_3^+$  and negatively charged fluoride ions. A similar observation was recorded by Huang et al<sup>26</sup>. Further, appearance of sharp peak at  $621\text{ cm}^{-1}$  and formation of broad peak at  $822\text{ cm}^{-1}$  after fluoride loading indicated the formation of  $\text{O...F}^{27}$  and  $\text{OH...F}^{28}$  bonds respectively. The IR

spectra (Fig 2c) of chromium loaded CPF showed perceptible changes in comparison with that of unused CPF more so in the region 600 to 1200. Two new peaks at 774 and 904  $\text{cm}^{-1}$ ,

attributed to the Cr–O and Cr=O bonds from the Cr(VI) species, appeared, which suggests that Cr(VI) was adsorbed on the surface of CPF<sup>29</sup>.

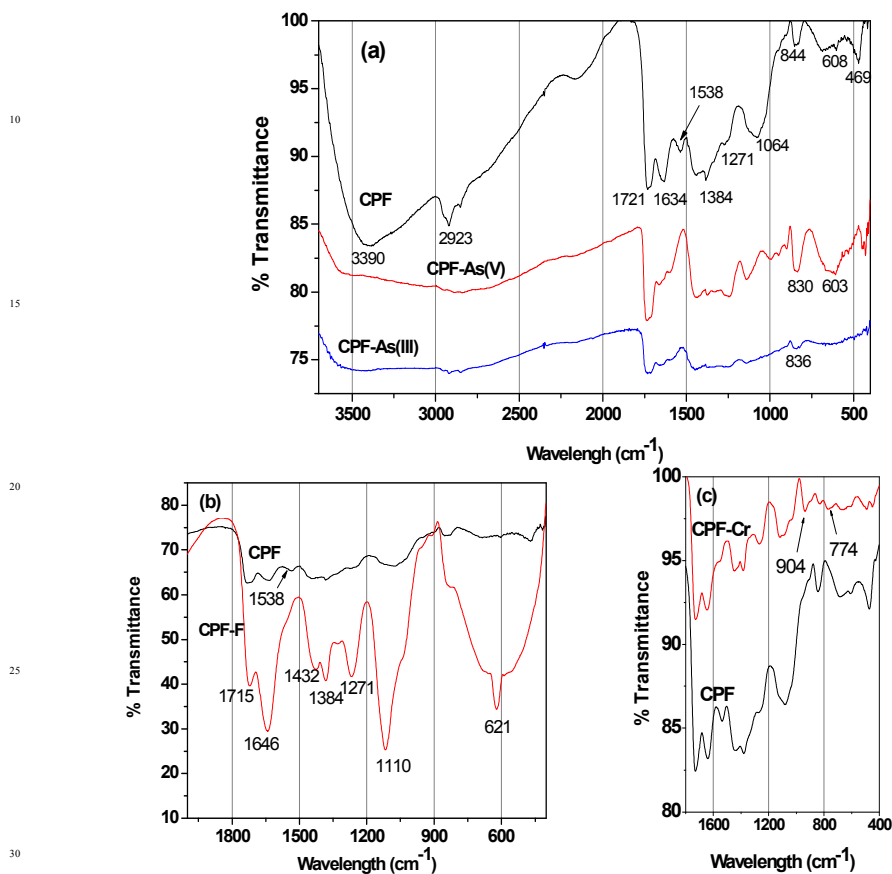


Fig.2 FTIR spectra of a. CPF and As(III) and As(V) loaded CPF, b. CPF and Fluoride loaded CPF, c. CPF and Cr(VI) loaded CPF

### 3.1.3 XRD Measurements

The X-ray diffraction (XRD) patterns of the virgin CPF and As(III) and As(V) loaded CPF nanofibres were recorded at ambient temperature. The samples were irradiated with monochromatized Cu KR (1.5406 Å) X-ray source and analyzed between  $10^\circ$  to  $70^\circ$  ( $2\theta$ ). The operating voltage and current used were 45 kV and 40 mA, respectively. Figure 3 revealed that the CPF nanofibrous membranes possessed one sharp diffraction peak at  $2\theta$  values around  $22.7^\circ$  and one broad diffraction peaks at  $40.1^\circ$ . The sharp peak corresponds to the reflection peak of electrospun Chitosan/PVA nanofibres<sup>30</sup> and the broad peaks around  $31.6^\circ$  and  $42^\circ$  corresponds to amorphous ferric oxide crystalline phases<sup>31</sup>. It is also evident from the figure that after arsenic loading distinct peaks appeared at  $60.9^\circ$  which could be attributed to the formation of ferric arsenate.<sup>32</sup>

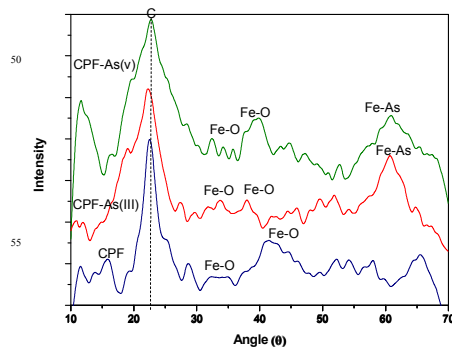


Fig.3 XRD patterns of CPF and As(III)/As(V) loaded CPF



### 3.2 Adsorption Experiments

Adsorption studies were carried out at room temperature to study the effect of adsorption time, and initial pH. For variation of pH experiments only initial pH of the aqueous solution was varied and efforts were not made to maintain the pH during the sorption experiments. The results obtained are shown in Fig. 3. In pH variation studies (Fig.3a) it is evident that maximum adsorption of Cr(VI) took place at pH 3. In the pH range of 2 to 5 the predominant Cr(VI) species is  $\text{HCrO}_4^-$ ,<sup>33</sup> which can chelate with Fe(III) present in the CPF mat via the ligand exchange mechanism<sup>34</sup>. In the case of arsenic, maximum adsorptions of both trivalent and pentavalent species are observed in the pH values between 6 to 7.5. It is reported that iron(III) oxides exist as cationic monomeric form of  $\text{Fe}(\text{OH})_2^+$  below pH 7<sup>35</sup>. Arsenate exists as  $\text{H}_2\text{AsO}_4^-$  or  $\text{HASO}_4^{2-}$  at pH values greater than 3 and arsenite exists as neutral species  $\text{H}_3\text{AsO}_3$  at pH values less than 9<sup>35</sup>. Though both arsenite and arsenate are removed from the solution by the formation of ferric arsenite and arsenate, the formation of ferric arsenate is more facilitated by the ionic attraction as evident from the pH results. Hence initially, ionic attraction takes place between anionic arsenate species and cationic ferric hydroxide, followed by ligand exchange reaction leading to ferric arsenate. A similar observation is reported by many researchers for arsenic removal by either iron oxide or iron coated materials<sup>35</sup>. Additionally, arsenate ions are attracted to protonated amino groups of chitosan by electrostatic attraction followed by reduction and complexation with protonated/deprotonated amino groups<sup>36</sup>. Further FTIR (Fig.2a) and XRD spectra (Fig.3) confirms the formation of ferric arsenate. It is apparent that maximum fluoride adsorption occurred at pH 7.5. Lower adsorption fluoride ions at pH < 7.5 could be attributed to the formation of hydrofluoric acid. Under alkaline conditions, decrease in fluoride uptake could be due to the competition from hydroxyl ions. From the pH studies it is evident that fluoride sorption takes place by the electrostatic attraction between the protonated amino groups of chitosan and fluoride ions. A similar observation has been observed elsewhere<sup>37</sup>. Further interaction of fluoride ions with hydroxyl groups of the chitosan by ion exchange or hydrogen bonding is also plausible. This is confirmed by the FTIR studies (Fig. 2(b)). Similarly in the case of arsenate and chromate electrostatic interaction between protonated amino groups of the chitosan and the anions is also possible. A schematic representation of the sorption of crosslinked chitosan mat with different ions studied is depicted in scheme 2.

Figure 3b. shows the time profile of As(III), As(V), Cr(VI) and F-adsorption by CPF in batch mode. From the results it is evident Cr(VI) sorption onto CPF is very fast and > 98% sorption was

observed within 30 min. For other ions complete equilibrium was achieved at equilibration time > 2.5 h. Obtained data was modeled by Ho's pseudo second order equation<sup>38</sup> given by

$$\frac{t}{qt} = \frac{1}{k_2' qe^2} + \frac{t}{qe} \quad (3)$$

Where  $k'$  the pseudo second-order rate constant of adsorption ( $\text{g}/\text{mg}/\text{h}$ )  $q_e$  and  $q_t$  are the amounts of analyte ion sorbed ( $\text{mg}/\text{g}$ ) at equilibrium and at time  $t$ , respectively. Linear plots of  $t/qt$  Vs  $t$  for the various ions yielded straight line with correlation coefficients of > 0.945. The calculated values of various constants are tabulated in Table 1.

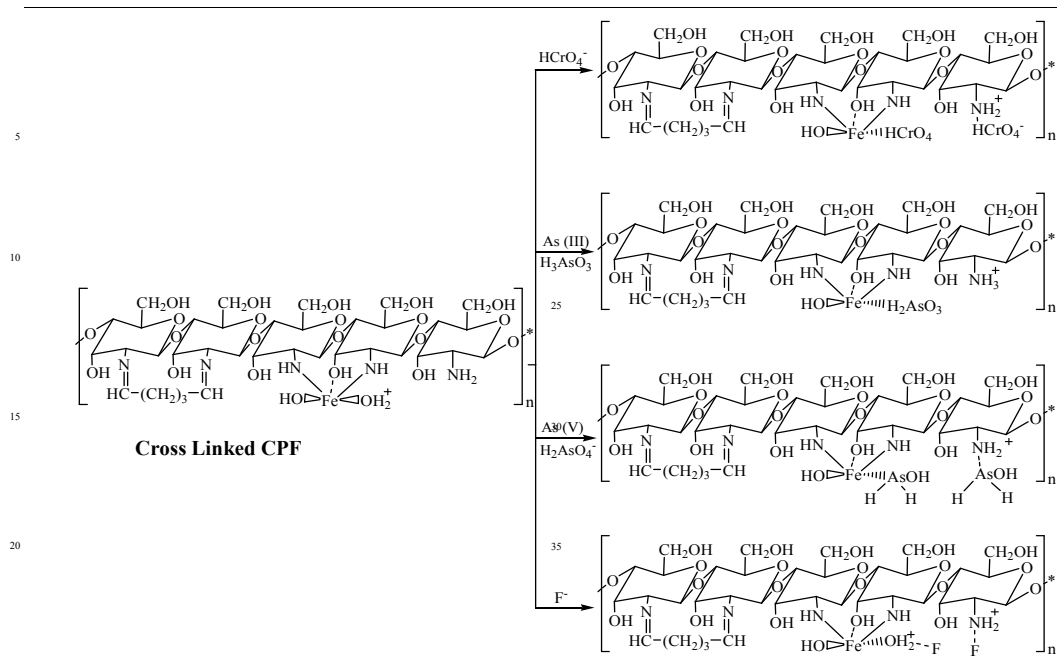
The equilibrium sorption isotherms of different ions were studied and the results obtained shown in Fig. 3c. The values were modeled using linearized Langmuir isotherm

$$1/q_e = 1/Q_b C_e + 1/Q \quad (4)$$

Where,  $q_e$  is the amount of solute adsorbed ( $\text{mg}/\text{g}$ ) at equilibrium and  $C_e$  is the equilibrium concentration ( $\text{mg}/\text{L}$ ). The empirical constants  $Q$  and  $b$  denote the monolayer capacity and energy of adsorption, respectively, and were calculated from the slope and intercept of plot between  $1/C_e$  and  $1/q_e$ . The values obtained are shown in Table 1. Maximum adsorption capacities of Cr(VI), As(V), As(III) and F were found to be 166.7, 83.3, 32.3 and 2.5  $\text{mg}/\text{g}$  respectively. The adsorption capacity obtained for Cr(VI) is higher than other reported sorbents like magnetic chitosan hydrogel (144.9  $\text{mg}/\text{g}$ )<sup>17</sup>, 2013, sugarcane bagasse (5.09  $\text{mg}/\text{g}$ )<sup>39</sup>, magnetic particles( $\text{Fe}_3\text{O}_4$ ) immobilized onto PEI/acrylate beads (109.2  $\text{mg}/\text{g}$ )<sup>40</sup>, alginate (42.6  $\text{mg}/\text{g}$ )<sup>41</sup>, activated carbon and Bacillus subtilis (19.43  $\text{mg}/\text{g}$ )<sup>42</sup>. In the case of arsenic species, it is observed that the adsorption capacity of CPF towards As(V) was 2.6 times higher than As(III). This could be attributed to the prevalent electrostatic attraction between anionic arsenic species and cationic surface charge of the sorbent, which aids the rapid complexation of arsenic with Fe(III) leading to the formation of ferric arsenate. Complexation of Fe(III) with arsenite or arsenate have been reported by other researchers<sup>12,16</sup>. It is also noteworthy that the adsorption capacity obtained for CPF towards arsenate removal was higher than the recently reported Fe(III) incorporated PVA nano fibres (36  $\text{mg}/\text{g}$  As(V))<sup>12</sup>, Zerovalent iron incorporated chitosan nanofibres (1.65 $\text{mg}/\text{g}$  As(III); 2.29  $\text{mg}/\text{g}$  As(V))<sup>15</sup>, chitosan/PVA nano fiber (1.68  $\text{mg}/\text{g}$  As(III); 0.56 As(V)  $\text{mg}/\text{g}$ )<sup>14</sup> and iron chitosan flakes (16.15  $\text{mg}/\text{g}$  As(III); 22.47  $\text{mg}/\text{g}$  As(V))<sup>16</sup>. Although the CPF nano fibre exhibited high capacity towards Cr(VI), As(III) and As(V) its capacity towards fluoride is comparatively less. The fluoride uptake capacity of CPF is comparable to the most commonly and widely used sorbent i.e. activated alumina (2.41  $\text{mg}/\text{g}$ )<sup>43</sup>.

Table 1 Langmuir Equilibrium Isotherm and Pseudo second order model constants

Analyte	Langmuir Isotherm Model			Pseudo Second order Model	
	$Q_b$ ( $\text{mg}/\text{g}$ )	$b$ ( $\text{L}/\text{mg}$ )	$R^2$	$k'$ ( $\text{g}/\text{mg}/\text{h}$ )	$R^2$
As(III)	32.3	0.082	0.99	1.304	0.94
As(V)	83.3	4.000	0.91	0.905	0.99
Cr(VI)	166.7	0.006	0.97	10.000	1.00
F	2.5	0.413	0.95	1.404	0.98



Scheme 2. Schematic representation of the mechanism of interaction of crosslinked CPF with As(III), As(V), Cr(VI) and F

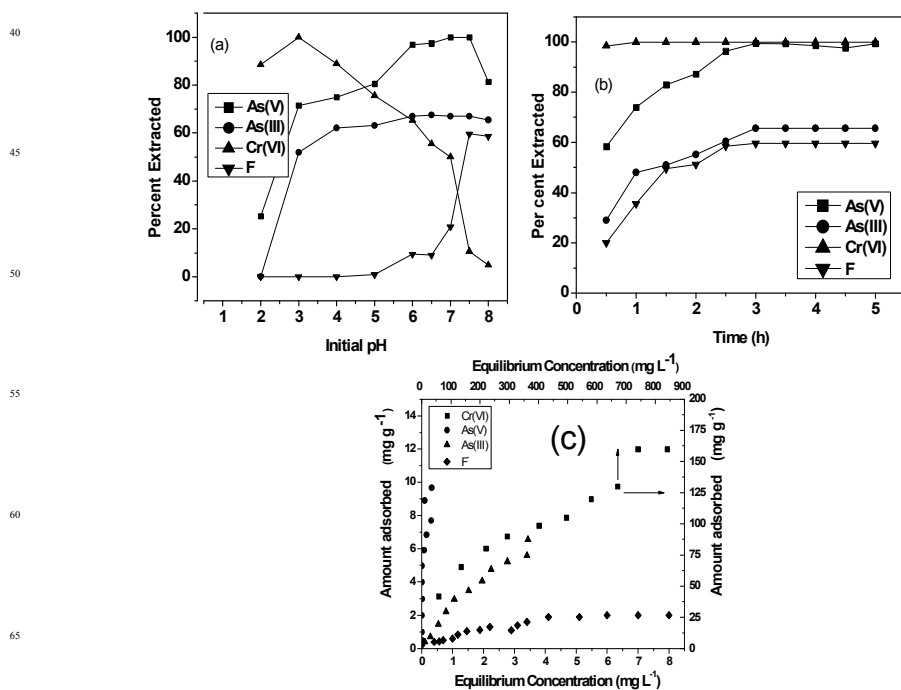


Fig.3 (a) Effect on initial pH on sorption (b) Kinetics plot (c) Equilibrium Isotherm Plots of Cr(VI), As(III), As(V) and F and CPF system

70

Cite this: DOI: 10.1039/c0xx00000x

www.rsc.org/xxxxxx

### 3.3 Selectivity Studies

Selectivity studies were conducted by equilibrating a mixture of 5 ppm each of Cr(VI), As(III), As(V) and F<sup>-</sup> in 100 ml with 0.1 g of CPF mat for 3 h at pH 7. After equilibration, the solutions were filtered and analyzed for the various ions. The selectivity performance of CPF are summarized in Fig.4. The selectivity order of the investigated anions towards CPF followed the sequence Cr(VI) > As(V) > As(III) > F<sup>-</sup>. It should be noteworthy thought the optimum pH for Cr(VI) adsorption is pH 3, around 90% sorption took place in pH 7.

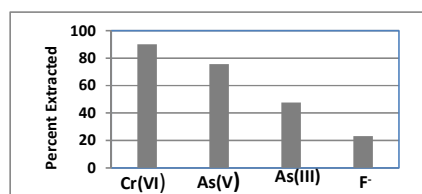


Fig.4 Selectivity Studies

### 3.4 Antibacterial activity

Figure 4 shows the test result of chitosan/pva (CP) and chitosan/pva/Fe (CPF) nanofibers mat against *E.coli* bacterial strain. The inhibitory effect of nano fibers were determined on the basis of number of colonies found in LB agar plate. As observed from figure that prepared CPF nanofibers mat had superior inhibitory effect compared to CP nanofibers mat against *E.coli*. It was also observed that inhibitory effect against *E. coli* bacterial strain increased with increased amount of prepared CPF mats. The larger amount (0.3 gm) of CPF nanofibers mat completely inhibited the bacterial colony at approximately 12 h, which showed the relatively superior performance. However, at lower amount (0.05 and 0.1 gm) of CPF mat showed gradually decrement in bacterial growth. In case of CP nanofibers mat, it is evident that mat has the capability to reduce bacteria only for 12 h and after 12 h the number of colonies increased with time. This observation is in accordance with earlier reports<sup>44</sup>. The inhibitory effect of CPF mat is due to the presence of chitosan and Fe metal prevalent in the mat. As mentioned earlier in the text, chitosan exhibited antibacterial activity against gram negative and gram positive bacterial strains due to the interaction of poly-cationic amines with negatively charged substances at the cell surface of bacteria<sup>7</sup>. While Fe metal also has bactericidal effect because of the generation of reactive oxidative stress that causes cellular disruption, which lead to the cell death<sup>45</sup>.

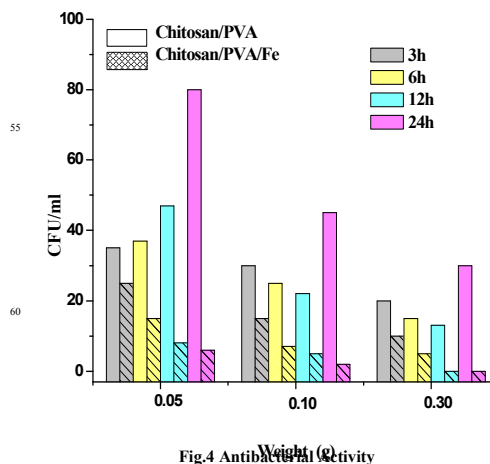


Fig.4 Antibacterial Activity

### 4. Conclusions

A novel nanofibrous composite mats consisting of chitosan/Fe(III)/PVA was synthesized by electrospinning technique. The prepared mats were stabilized by crosslinking with glutaraldehyde and characterized by various techniques. The versatility of the mat was demonstrated by their high sorption capacity towards various toxic anions such as As(III), As(V), Cr(VI) and F<sup>-</sup>. The equilibrium data were modeled using Linearized Langmuir model and the adsorption capacities of Cr(VI), As(III), As(V) and F<sup>-</sup> were found to be 166.7, 83.3, 32.3 and 2.5 mg/g respectively. Further the CPF mat exhibited disinfection control towards *e. coli* bacteria. Thus, removal of both toxic contaminants coupled with antibacterial activity makes CPF nanofibrous mats a promising candidate in pure drinking water sector.

### Notes and references

<sup>a</sup> Centre for Environmental Science and Engineering, Indian Institute of Technology Kanpur, Kanpur, U.P. 208016, India

<sup>b</sup> Department of Chemistry, Banasthali Vidyapith Rajasthan 304022, India

\*Author for Correspondence  
Email: [nalmi@iitk.ac.in](mailto:nalmi@iitk.ac.in) Tel: +91915122596360

- Escher, B. I., Fenner, K. *Environ. Sci. Technol.*, 2011, **45**, 3835.
- EPA National Primary Drinking Water Standards 2009. <http://www.epa.gov/safewater/contaminants/index.html> for more information
- Gupta, S. S., Bhattacharyya, K. G., *Adv. Colloid Interface Sci.*, 2011, **162**, 39.
- Fu, F., Wang, Q., *J. Environ. Manage.*, 2011, **92**, 407.

5. Pillay, K., Cukrowska, E.M., Coville, N.J., *J. Hazard Mater.* 2009, **166**, 1067.
6. Guibal E. *Separation and Purification Technology*, 2004, **38**, 43.
7. Angelova, N.M., Rashkov, I., Maximova, V., Bogdanova, S., Domard, A., *J Bioact Compat Pol.*, 1995, **10**, 285-298.
8. Desai, K., Kit, K., Li, J.J., Davidson, P.M., Zivanovic, S., Meyer, H., *Polymer*. 2009, **50** 3661.
9. Haider S., Park S.Y., *J. Membr. Sci.* 2009, **328**, 90.
10. Bjorge, D., Daels, N., Vrieze, S.d., Dejans, P., Camp, T.V., Audenaert, W., Hogie, J., Westbroek, P., Clerck, K.D., Hulle, S.W.H., *Desalination*, 2009, **249**, 942.
11. Lala, N.L., Ramaseshan, R., Li, B., Sundarajan, S., Barhate, R.S., Liu, Y.J. and Ramakrishna, S., *Biotechnol. Bioeng.* 2007, **97**, 1357.
12. Mahanta, N. and Valiyaveetil, S., *RSC Adv.* 2013, **3**, 2776.
13. Horzum, N., Demir, M. M., Nairate, M., Shahwan, T., *RSC Adv.* 2013, **3**, 37828.
14. Chauhan, D., Dwivedi, J., Sankaramakrishnan, N., *Env. Sci.Polln.Res.*, (2014), DOI 10.1007/s11356-014-2864-1.
15. Zhang, Y., Huang, X., Duan, B., Wu, L., Li, S., Yuan, X., *Colloid Polym. Sci.* 2007, **285** 855.
16. Gupta, A., Chauhan, V.S., Sankaramakrishnan, N., *Water Res.* 2009, **43**, 3862.
17. Yu, Z., Zhang, X., and Huang, Y., *Ind. Eng. Chem. Res.* 2013, **52**, 11956.
18. Tang, C., Saquing, C.D., Harding, J. R. and Khan, S. A., *Macromolecules*. 2010, **43**, 630.
19. APHA (1998). Standard Methods for the Examination of Water and Wastewater, 20th edition. American Public Health Association, Washington, D.C.
20. Deitzel, J.M., Kleinmeyer, J., Harris, D., Tan, N.C.B., *Polymer*, 2001, **42**, 261.
21. Meng, Z.X., Zheng, W., Li, L., Zheng, Y.F., *Mater.Chem.Phys.* 2011, **125**, 606.
22. Jia, Y.T., Gong, J., Gu, X.H., Kim, H.Y., Dong, J., Shen, X.Y., *Carbohydr polym.* 2007, **67**, 403.
23. Amonette, J.E., Rai, D., *Clays and clay minerals*, 1990, **38**, 129.
24. Sankaramakrishnan, N, Gupta, A, Vidyarthi, S.R., *J. Environ. Chem. Engg.*, 2014, **2**, 802.
25. Jia, Y., Liying, X., Wang, X., Demopoulos, G.P., *Geochim.Cosmochim.Acta.*, 2007, **71**, 1643.
26. Huang, R., Yang, B., Liu, Q., Ding, K., *J. Fluorine Chem.*, 2012, **141**, 29.
27. Raul, P.K., Devi, R.R., Umlong, I.M., Banerjee, S., Singh, L., Purkhait, M., *J.Nanosci.Nanotechnol.*, 2012, **12**, 3922.
28. Sundaram, C. S., Viswanathan, N., Meenakshi, S., *J. Hazard. Mater.* 2008, **155**, 206
29. Sankaramakrishnan, N., Dixit, A., Iyengar, L., Sanghi, R., *Bioresource Technol.*, 2006, **97**, 2377.
30. Jia, Y.T., Gong, J., Gu, X.H., Kim, H.Y., Dong, J., Shen, X.Y., *Carbohydr polym.* 2007, **67**, 403.
31. Swiatkowska-Warkocka Z, Kawaguchi K, Wang H, Katou Y, Koshizaki N, *Nanoscale Res Lett* 2011, **6**, 226.
32. Jia, Y., Xu, L., Wang, X., Demopoulos, G. P., Infrared spectroscopic and X-ray diffraction characterization of the nature of adsorbed arsenate on ferrihydrite, *Geochim. Cosmochim. Acta*, 2007, **71**, 1643.
33. Dionex, 1998, Technical note 26 LPN 034398-02 1M 1/98. [Online] Available at: [http://www.dionex.com/enus/webdocs/4428TN26\\_16May07\\_LPN034398-02.pdf](http://www.dionex.com/enus/webdocs/4428TN26_16May07_LPN034398-02.pdf).
34. Zimmermann, A.C, Mecabó, A., Fagundes, T., Rodrigues, C. A., *Jl. Haz. Mat.*, 2010, **179**, 192.
35. Katsoyiannis, I.A., Zouboulis, A.I., *Water Res.*, 2002, **36**, 5141.
36. Man, K.C., Ph.D. Thesis, Hong Kong University of Science and technology, 2009.
37. Petrusovski, B., Sharma, S., Schippers, J.C. and Shordt, K., IRC International Water and Sanitation Centre; 2007.
38. Ho, Y.S., McKay, G, *Process Biochem.*, 1999, **34**. 451.
39. Alomá, C., Rodríguez, I., Calero, M., Blázquez, G., Desalination and Water treatment, 2013, DOI: 10.1080/19443994.2013.812521.
40. Bayramoglu G., Arica M.Y., *Chem. Eng. J.* 2008, **139**, 20.
41. Bertagnolli, C., da Silva, M. G. C., Guibal, E., *Chem. Eng. J.*, 2014, **237**, 362.
42. Sukumar, C., Gowthami, G., Nitya, R., Janaki, V., Kannan, S. K., Shanthi, K., *Environ Earth Sci.*, 2013, DOI 10.1007/s12665-013-3007-6.
43. Chauhan, V.S., Dwivedi, P.K., Iyengar, L., *J. Hazard. Mater.*, 2007, **139**, 103.
44. Jeon, S.J., Oh, M., Yeo W-S, Galvao, K.N, Jeong K.C., *Plos one*, 2014, **9**, e92723.
45. Inbaraj, B. S., Tsai T.-Y and Chen B.-H., *Sci. Technol. Adv. Mater.*, 2012, **13**, 1.

---

5  
10  
15  
20  
25

RSC Advances Accepted Manuscript